Strojniški vestnik - Journal of Mechanical Engineering 62(2016)2, 127-136
DOI:10.5545/sv-jme.2015.2837
Original Scientific Paper
Received for review: 2015-07-09
Received revised form: 2015-10-20
Accepted for publication: 2015-12-17

Design and Analysis of Double-side Meshing and Dual-phase Driving Timing Silent Chain System

Yabing Cheng* – Shuaibing Yin – Xiaopeng Wang – Lichi An – Huan Liu
Jilin University, School of Mechanical Science and Engineering, China

Based on the structure of automotive engines and the layout of their timing system, the timing silent chain system including the overall layout, the structure of link plate and sprockets, and chain length are designed. The design method of double-side meshing and dual-phase driving timing silent chain system is presented. A dynamic analysis model is built, and the fluctuation of the tension sprocket, and the vibration of the system, and the rotation speed stability of exhaust camshaft sprocket, and the transmission error of the intake camshaft sprocket and exhaust camshaft sprocket, and the contact force between the link plate and other components are analysed. Furthermore, dynamic characteristics of the system are contrasted with a single-phase timing silent chain system. Analysis results show that the double-side meshing and dual-phase driving timing silent chain system has a distinct advantage in reducing vibration and enhancing driving stability. The system designed in this paper can meet the requirements of engine timing system, which further verifies the scientific validity and effectiveness of the design method of the double-side meshing and dual-phase driving timing silent chain system proposed in this paper.
Keywords: design method, double-side meshing, dual-phase driving, timing silent chain system, dynamic characteristics

Highlights
- *Established the geometric model of link plate and sprockets.*
- *Presented systematic design method of double-side meshing and dual-phase driving timing silent chain system.*
- *Designed a double-side meshing and dual-phase driving timing silent chain system.*
- *Studied the dynamic characteristics of the system.*
- *The double-side meshing and dual-phase driving timing silent chain system have better performance than a single-phase driving timing silent chain system.*

0 INTRODUCTION

The engine timing system is a core component to ensure normal operation of automotive engines. Recently, with the rapid development of the auto industry, timing chains have increasingly been used in engine-timing systems instead of timing belts or gear transmissions. However, only a few enterprises, such as BorgWarner and DID, own most of the key technologies and patents about new type automobile engine timing chains. Because of business secrecy, only a few references are available. Thus, many enterprises encounter technical barriers in the production of high-quality timing chains.

Research on the chain-driving system has been conducted by many scholars and experts. Based on the link plate-sprocket-hob meshing mechanism, Meng et al. [1] introduced the choice and calculation method for the chain, analysed the working condition and the main loss of effectiveness form of automobile chain, proposed multi-variant variation design method, and examined the effects of the testing temperature and fluctuant speed on the wear resistance of the new silent chain [2] to [3]. Chintien et al. [4] investigated the relative motion between the sprocket and a link plate from the tight span stage to the seated stage. Xu et al. [5] developed a mathematical model to calculate the dynamic response of a roller chain drive working at a constant or variable speed condition. Troedsson and Vedmar [6], researched the oscillations in a chain drive under different speeds using dynamic analysis. Pereira et al. [7], built chain drive automatic multibody models from a minimal set of data, and aimed to overcome the difficulty of building manually complex models of chain drives. Wang et al. [8] designed a new sprocket tooth profile to reduce the polygonal action and meshing impact. Zhang [9] analysed the transverse vibration of an axially moving silent chain by using multi-body dynamics. Xue et al. [10] to [11], researched the design and manufacture of the involute sprocket through CAD software, and studied the engagement theory of the involute sprocket by the engagement analysis between the silent chain and involute sprocket. Pedersen and Hansen et al. [12] and Pedersen [13] developed a dynamic model of a roller chain drive including the impact of guide bars, the inner friction and polygonal action of roller chains. Cheng et al. [14] proposed a design method of the dual-phase Hy-Vo silent chain transmission and studied the polygon effect through mathematical analysis.

Recently, with the increase of individualized needs, the research on timing silent chains has been varied, including meshing mechanism variation,

*Corr. Author's Address: Jilin University, School of Mechanical Science and Engineering, Renmin street 5988 , Changchun, China. chengyb@jlu.edu.cn

shape variation, and parameter variation. Meshing mechanism variation includes outer meshing, inner-outer compound meshing, and outer meshing with inner-outer compound meshing. Shape variation includes pinhole shape variation, shape variation of the pin cross section, and guide plate shape variation. Parameter variation includes the variation of positioning offset angle, the apothem, the plate tooth profile angle, and sprocket pressure angle. However, all the silent chains researched in the above papers are single-side meshing chains based on a single-phase chain driving system. In this paper, a double-side meshing and dual-phase driving timing silent chain system are designed, the system is established, and the design method of the system is put forward. Through dynamic simulation, the rationality and scientific validity of the design method of the double-side meshing and dual-phase driving timing silent chain system are verified, and the advantages of the system are revealed.

1 ESTABLISHMENT OF THE TIMING SILENT CHAIN SYSTEM STRUCTURE

As shown in Fig. 1, the timing silent chain system designed in this paper is composed of a crankshaft sprocket, intake camshaft sprocket, exhaust camshaft sprocket, sprocket tension group, idle gear group A, idle gear group B, and timing chains. The crankshaft sprocket, intake camshaft sprocket, and exhaust camshaft sprocket are dual-phase sprockets.

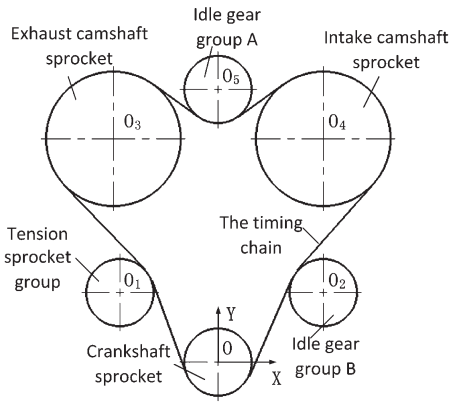

Fig. 1. *The structure of timing silent chain system*

The structure of the dual-phase sprocket is shown in Fig. 2. It is composed of two connected identical sprockets, and the two sprockets have a phase difference of π/z, where z is the tooth number of the sprocket. The tension sprocket group, idle gear group A, and idle gear group B have the same structure, and they all consist of a pair of coaxial single-phase sprockets, which can rotate without interference. The structure of the single-phase sprocket is shown in Fig. 3, and the assembly diagram of the idle sprocket groups is shown in Fig. 4. The crankshaft sprocket is the driving wheel, and has 19 teeth. The intake camshaft sprocket and the exhaust camshaft sprocket are driven wheels, and it has 38 teeth. There are two timing chains with the same length in the system, and each chain meshes with one sprocket of the sprocket groups. This design ensures that the sprocket tension group and idle gear groups can work more efficiently and minimize the vibration of the system.

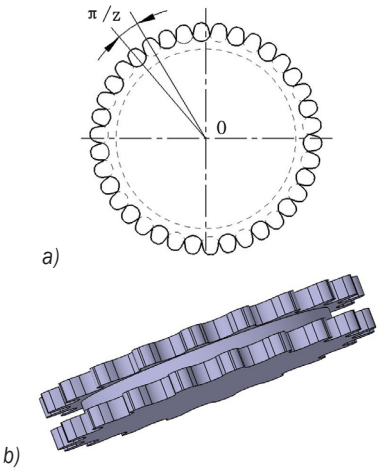

Fig. 2. *Schematic diagram of the dual-phase sprocket; a) Front view, b) side view*

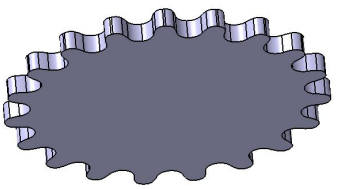

Fig. 3. *Schematic diagram of the single-phase sprocket*

The coordinate system is established as shown in Fig. 1. The crankshaft sprocket centre is regarded as the coordinate origin, and the horizontal direction is regarded as the *X*-axis, and the vertical direction is regarded as the *Y-axis*. The intake camshaft sprocket and exhaust camshaft sprocket are symmetrical about the *Y-axis*. The coordinate of the exhaust camshaft sprocket centre is (–75,160), and the coordinate of intake camshaft sprocket centre is (75,160). To ensure the stability of the driving, the centre distance between the driving sprocket and driven sprocket is usually 30 to 50 times that of the chain pitch. In order to reduce engine vibration and noise, sprocket tension group is

installed on the loose side, and idle gear group B is installed on the tight side.

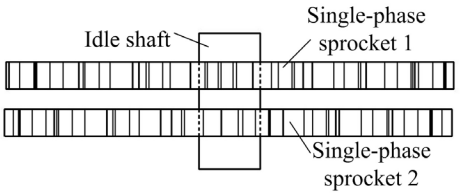

Fig. 4. *Assembly diagram of sprocket tension group and idle sprocket groups*

2 GEOMETRIC MODEL ESTABLISHMENT OF THE DOUBLE-SIDE MESHING AND DUAL-PHASE DRIVING TIMING SILENT CHAIN SYSTEM

2.1 Geometric Model Establishment of the Link Plate

Fig. 5 shows the structure of the link plate. The link plate is an inner and outer compound mechanism that can further reduce the fluctuation of the system [15]. Supposing that A is the hole pitch of the link plate, f is the benchmark apothem between the circle centre O and link plate outside linear profile, 2α is the tooth profile angle of the link plate, h is the distance between the centreline and the crotch of the link plate, r is the curvature radius of inner tooth profile, and $O_1(x_1,y_1)$ is the central coordinate of it. When the chain is straightened, the medial profile overhang of the link plate is δ.

The crankshaft sprocket, tension sprockets, and idle gears have the same number of teeth. The basic pitch of the double-side meshing chain is $p=8$ mm, the gap between the pinhole and the pin is $\Delta=0.04$ mm, $A=p-\Delta=7.96$ mm, $\delta=0.217$ mm, $\alpha=30°$, $r=13.37$ mm, $h=1.4$ mm. When the link plate is a broad waist link plate, $f=0.40$, $p=3.2$ mm.

The coordinate of the inside tooth profile curvature centre is calculated as:

$$\begin{cases} x_1 = \dfrac{r-f-\delta}{\cos\lambda}\sin\left(\lambda+60°\right) \\ y_1 = \dfrac{r-f-\delta}{\cos\lambda}\cos\left(\lambda+60°\right) \end{cases}, \quad (1)$$

where $\lambda = \arctan(x_1/y_1)-60°=10°$.

According to Eq. (1), $x_1=9.513$ mm, $y_1=3.463$ mm can be obtained.

At the onset of the meshing, the inside convex flank of the link plate contacts the sprocket first. With the relative rotation of the link plate with the adjacent link plate, the engagement point transfers from the inside flank of the link plate to the outside flank of the adjacent link plate, and the inner-outer compound meshing is completed. Because of the symmetry of the link plate, the meshing process is exactly the same when the two sides of the link plate mesh with the sprockets. This meshing mechanism reduces the meshing impact between link plates and sprockets, relieves vibration, and improves the wear resistance of the system.

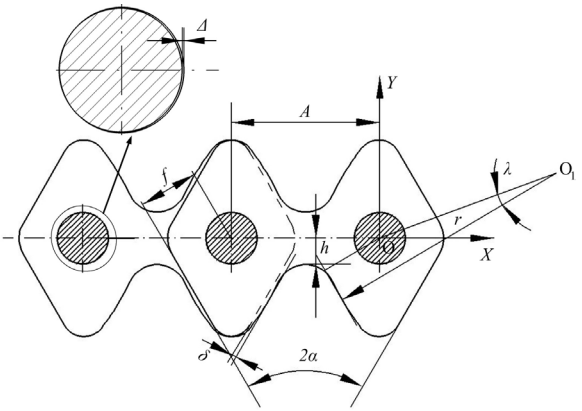

Fig. 5. *The structure of the double-side meshing link plate*

2.2 Establishment of the Geometric Model of the Sprockets

Fig. 6 shows the meshing diagram of link plates with a dual-phase sprocket. Involute tooth sprockets are designed to reduce the impact between the link plates and sprockets. Moreover, it will lead to a lower impact velocity and a higher wear resistance of the sprockets. Supposing p_0 is the initial pitch of the silent chain, f_0 is the initial apothem. p_2 is the normal pitch of hob, and normal tooth form angle of the hob is α_2 which is equal to α. σ is the phase difference of the sprocket, d_j is the pitch circle diameter of the sprocket, and d is the reference diameter of the sprocket. x is the modification coefficient of the hob, straight line k–k is the reference line of the hob before modification, and straight line e–e is the reference line of the hob after modification. Therefore, x is a minus, and the distance between e–e and k–k is $-xm_2$. As shown in the diagram, dotted lines stand for one phase of the system, while full lines stand for another phase. dR is the diameter of the gauge pin.

2.2.1 The Parameters of Crankshaft Sprocket

The tooth number of the crankshaft sprocket is $z=19$. When the tooth number of the sprocket is too small, a slight pressure angle of the sprocket will make the

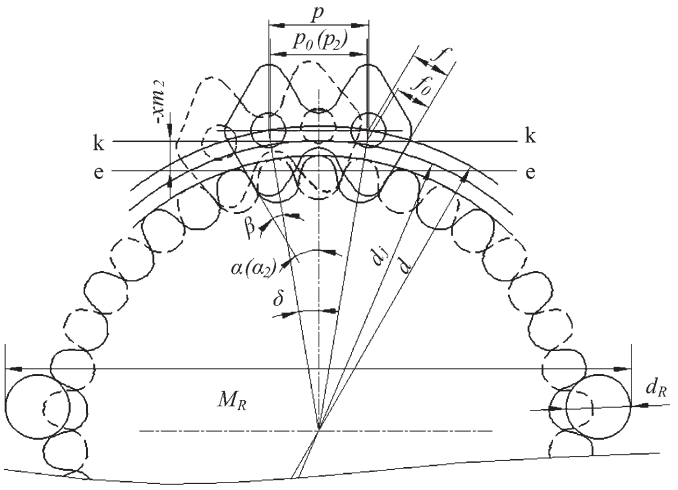

Fig. 6. *The design system of the double-side meshing and dual-phase driving silent link plate- sprocket–hob*

tooth root fragile. Thus, the sprocket pressure angle is set as 36°. The normal pitch of the hob is $p_2=p_0=7.455$ mm, and the normal tooth form angle of the hob is $\alpha_2=\alpha=30°$. The pitch of the crankshaft sprocket is $p_1=(p_2\cdot\cos\alpha_2)/\cos\alpha_1=7.98$ mm. The pitch increment is $\Delta p=p-p_0=0.545$ mm. When $\alpha=30°$, the side-heart distance increment is $\Delta f=\left[\cot(\pi/z)-\sqrt{3}\right]\Delta p/4=0.581$ mm. The initialized side-heart distance is $f_0=f-\Delta f=2.619$ mm. Thus, the modification coefficient of the hob is calculated as:

$$x=\frac{\pi\cot\alpha_2}{4}-\frac{z}{2}+\frac{\pi}{2\tan\frac{\pi}{z}}-\frac{\pi f_0}{p_2\sin\alpha_2}. \quad (2)$$

The measured distance is calculated as:

$$M_R=\frac{p_0}{\sin\left(\frac{\pi}{z}\right)}\cos\frac{\pi}{2z}+d_R, \quad (3)$$

where d_R is 5 mm.

According to Eqs. (2) and (3), $x=-0.938$, $M_R=50.138$ mm, can be obtained.

The phase difference of the sprocket is $\sigma=\pi/z=9.474°$. Since the tooth number of the tension sprockets and the tooth number of the idle sprockets are equal to the tooth number of the crankshaft sprocket, their parameters are equal to those of the crankshaft sprocket.

2.2.2 The Parameters of Intake Camshaft Sprocket and Exhaust Camshaft Sprocket

The parameters of the intake camshaft and exhaust camshaft are equal. Tooth number is $z=38$, the sprocket pressure angle is $\alpha_1=31.5°$, the normal pitch of hob is $p_2=p_0=7.876$ mm, and the normal tooth form angle of the hob is $\alpha_2=\alpha=30°$. The pitch of camshaft sprocket is $p_1=(p_2\cdot\cos\alpha_2)/\cos\alpha_1=8$ mm. The pitch increment is $\Delta p=0.124$ mm. When $\alpha=30°$ the side-heart distance increment is $\Delta f=\left[\cot(\pi/z)-\sqrt{3}\right]\Delta p/4=0.320$ mm, $f_0=2.520$ mm, $x=-0.703$, $M_R=100.293$ mm, $\sigma=\pi/z=4.737°$.

2.3 Position Calculation of Tension Sprocket Group and Idle Gear Groups

As shown in Fig. 7, the loose side concave distance C_2 is C_1, and the tight side concave distance C_2 is C_1. When the centre distance between the sprockets is small, and the transmission is horizontal or approximately horizontal, $C_1=(5\%\text{ to }8\%)a$, $C_2=(2\%\text{ to }5\%)a$ is. When the centre distance between the sprockets is large, and the transmission is vertical or nearly vertical, $C_1=(8\%\text{ to }12\%)a$, $C_2=(5\%\text{ to }8\%)a$ [1].

$O(x,y)$ is the centre of the crankshaft sprocket, $O_1(x_1,y_1)$ is the centre of the tension sprocket group, $O_2(x_2,y_2)$ is the centre of the idle sprocket group B, $O_3(x_3,y_3)$ is the centre of the exhaust camshaft sprocket, $O_4(x_4,y_4)$ is the centre of the intake camshaft sprocket, and $O_5(x_5,y_5)$ is the centre of the idle sprocket group A. Pitch circle radiuses of

the sprockets are r, r_1, r_2, r_3, r_4, r_5 respectively, and $r = r_1 = r_2 = r_5 = 24.438\,\text{mm}$, $r_3 = r_4 = 48.438\,\text{mm}$.

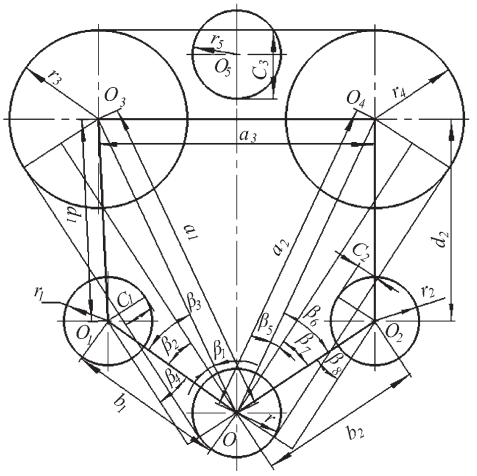

Fig. 7. *The design diagram of the system layout*

2.3.1 Position Calculation of Tension Sprocket Group

As shown in Fig. 7, the coordinate of O is $(0, 0)$, and the coordinate of O_1 is $(-75, 160)$. It can be ascertained that the centre distance between the crankshaft sprocket and the exhaust camshaft sprocket is $a_1 = \sqrt{(x_3 - x)^2 + (y_3 - y)^2} = 176.706\,\text{mm}$, and $C_1 = (8\,\%\,\text{to}\,12\,\%)a_1$.

According to Fig. 7, an equation set can be obtained:

$$\begin{cases} b_1 = \sqrt{(x_1 - x)^2 + (y_1 - y)^2} \\ d_1 = \sqrt{(x_3 - x_1)^2 + (y_3 - y_1)^2} \\ \sin\beta_1 = \dfrac{r_3 - r}{a_1} \\ \cos\beta_2 = \dfrac{a_1^2 + b_1^2 - d_1^2}{2a_1 b_1} \\ \beta_4 = \beta_2 = \beta_3 - \beta_1 \\ C_1 = r_1 - b_1 \sin\beta_4 + r \end{cases}. \quad (4)$$

According to Eq. (4), $O_1(-75, 50)$ and $C_1 = 17.538\,\text{mm}$ can be obtained to satisfy the equation set.

2.3.2 Position Calculation of Idle Sprocket Group B

As shown in Fig. 7, the coordinate of O is $(0, 0)$, and the coordinate of O_4 is $(75, 160)$. It can be ascertained that the centre distance between crankshaft sprocket and intake camshaft sprocket is $a_2 = \sqrt{(x_4 - x)^2 + (y_4 - y)^2} = 176.706\,\text{mm}$, and $C_2 = (5\,\%\,\text{to}\,8\,\%)a_2$.

According to Fig. 7, an equation set can be obtained:

$$\begin{cases} b_2 = \sqrt{(x_2 - x)^2 + (y_2 - y)^2} \\ d_2 = \sqrt{(x_4 - x_2)^2 + (y_4 - y_2)^2} \\ \sin\beta_5 = \dfrac{r_4 - r}{a_2} \\ \cos\beta_6 = \dfrac{a_2^2 + b_2^2 - d_2^2}{2a_2 b_2} \\ \beta_8 = \beta_7 = \beta_6 - \beta_5 \\ C_2 = r_2 - b_2 \sin\beta_8 + r \end{cases}. \quad (5)$$

According to Eq. (5), $O_2(75, 50)$ and $C_2 = 12.880\,\text{mm}$ $C_2 = 12.880\,\text{mm}$ can be obtained to satisfy the equation set 29.45°.

2.3.3 Position Calculation of Idle Sprocket Group A

As shown in Fig. 7, the centre distance between the exhaust camshaft sprocket and intake camshaft sprocket is $a_3 = \sqrt{(x_4 - x_3)^2 + (y_4 - y_3)^2} = 150\,\text{mm}$. Owing to the effect of gravity, the chain between the exhaust camshaft sprocket and intake camshaft sprocket hangs down badly. Therefore, C_3 should be large enough. The coordinate of point O_5 can be set as $(0, 195)$, and $C_3 = 37.74\,\text{mm}$ can be obtained.

2.4 The Length Calculation of the Silent Chain

As shown in Fig. 8, the length of the silent chain is composed of the lengths of six arcs and the lengths of six straight lines. According to Fig. 8, an equation set can be obtained:

$$\begin{cases} f_1 = \sqrt{b_1^2 - (r_1 + r)^2} \\ f_2 = \sqrt{d_1^2 - (r_1 + r_3)^2} \\ \beta_9 = \beta_{10} - \beta_{11} - \beta_{12} \\ \beta_{10} = \arccos\left(\dfrac{b_1^2 + d_1^2 - a_1^2}{2b_1 d_1}\right) \\ \beta_{11} = \arccos\left(\dfrac{r + r_1}{b_1}\right) \\ \beta_{12} = \arccos\left(\dfrac{r_1 + r_3}{d_1}\right) \end{cases}. \quad (6)$$

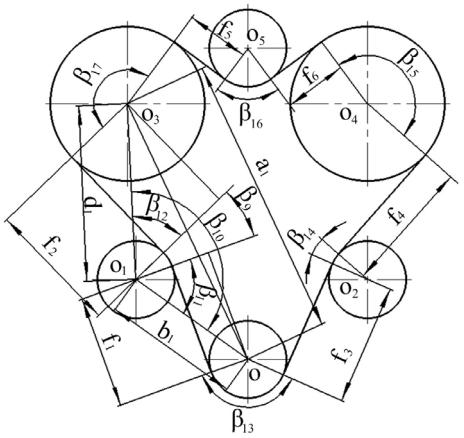

Fig. 8. *The diagram of chain length calculation*

According to Eq. (6), $\beta_9 = 23.88°$, $f_1 = 70.98$ mm, $f_2 = 82.67$ mm, can be obtained. Similarly, the values of $f_3, f_4, f_5, f_6, f_{13}, f_{14}, f_{15}, f_{16}, f_{17}$ can be obtained. Since $r = r_1 = r_2 = r_5$, $r_3 = r_4$, it can be ascertained that the length of the chain can be calculated as:

$$S = (\beta_9 + \beta_{13} + \beta_{14} + \beta_{17}) \times r + (\beta_{15} + \beta_{16}) \times r_3 + \\ + (f_1 + f_2 + f_3 + f_4 + f_5 + f_6). \quad (7)$$

Moreover, the link number is calculated as:

$$L = S / P. \quad (8)$$

According to Eqs. (7) and (8), L = 96.1 can be obtained. Considering the gaps between adjacent links, L should be larger than the exact value and be an even number. By adjusting the position of the sprocket tension group and the initial phase of all the sprockets, it can be ascertained that the link number of the system is $L = 98$.

3 DYNAMIC SIMULATION OF THE TIMING SILENT CHAIN SYSTEM

As shown in Fig. 9, based on the design parameters above, a dynamic model is established based on *RecurDyn* dynamic simulation software in which the decoupling algorithm of implicit numerical integration is used. In the system, a rigid body contact model is used, and all the components in the system are rigid bodies whose stiffness is close to infinity. The dynamic model is simplified in this paper, taking no account of the chain moving along the sprocket axial direction and the friction of the system. The timing silent chain is simplified to 1×1 form, and the pin length is more than 2 times the thickness of the link plate.

As for a 4-cylinder and 4-stroke engine, the load torque on the exhaust camshaft sprocket is a sine function of the rotation angle of the camshaft sprocket, and it goes through four cycles while the exhaust camshaft sprocket takes a turn. According to the principles of the engine valve system, intake camshaft sprocket is also a sine function only with a phase difference about exhaust camshaft sprocket, and the phase difference is 1/4 of the period T. Therefore. the functions between load torque, and the rotation angle of camshaft sprockets can be established. It can be ascertained that the period of the load torque is $T = 2\pi/4 = \pi/2$, the frequency is $\omega = 2\pi/T = 4$, the phase difference between exhaust camshaft sprocket and exhaust camshaft sprocket is $\varphi = T/4 = \pi/8$. Moreover, for the convenience of research, amplitude A and initial torque B can be valued as $A = 10$ and $B = 2$. Therefore, it can be obtained that the load torque exerted on the exhaust camshaft sprocket is $M_1 = (10 \times \sin(4\theta + \pi/8) + 2)$, and the load torque exerted on the intake camshaft sprocket is $M_2 = (10 \times \sin(4\theta) + 2)$. As shown in Fig. 10, curve 1 represents M_1 and curve 2 represents M_2, where θ is the rotation angle of the camshaft sprocket.

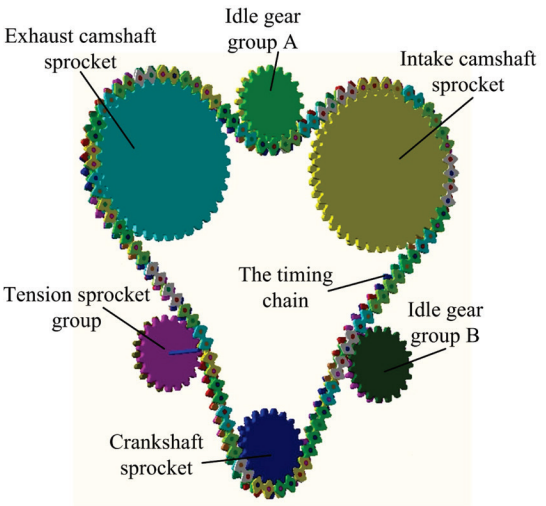

Fig. 9. *The simulation model of double-side meshing and dual-phase driving timing silent chain system*

After simulation, the result can be obtained through *Plot Result* in *RecurDyn*. The fluctuation of tension sprocket, the vibration of the chain system, the rotation speed stability of exhaust camshaft sprocket, the transmission ratio of the intake camshaft sprocket and exhaust camshaft sprocket, and contact force between link plate and other components are analysed when the crankshaft sprocket rotation speed is $n = 2000$ r/min. As shown in Fig. 11, the input driving

on the crankshaft sprocket is *step* (*time*, 0, 0, 0.05, –66.7×π). Furthermore, the simulation results of the dual-phase silent chain system and single-phase silent chain system are compared.

Tension sprockets move along a straight line, and the angle between the line and X axis is 36.2°. Thus, the fluctuation of tension sprockets can be obtained by measuring the fluctuation along the X axis. Due to the existence of the assembly gap, the fluctuation is serious during the initial stage of the running. Take the period of 0.11 s to 0.18 s to study the fluctuation when the system is approximately steady, and the fluctuation curve is shown in Fig. 12.

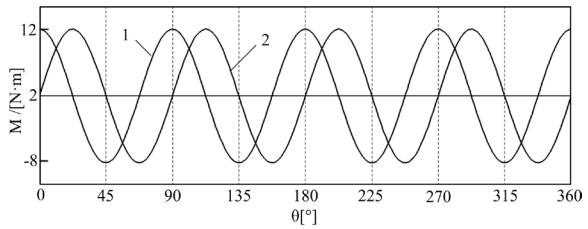

Fig. 10. *Load torque on the camshaft sprockets*

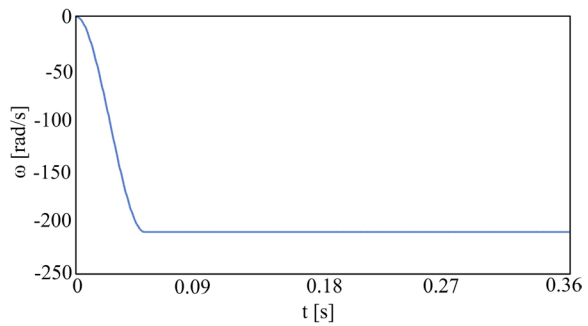

Fig. 11. *Input driving on the crankshaft sprocket*

3.1 Fluctuation Analysis of Tension Sprocket

As shown in Fig. 12, I is the fluctuation of single-phase silent chain system, and II is the fluctuation of the dual-phase silent chain system. The minimum value and maximum value of curve I is A(–60.131) and B(–60.058). The minimum value and maximum value of curve II are C (–60.119) and D (–60.072). y_A, y_B, y_C, y_D are respectively the y-direction ordinates of point A, B, C, and D. Thus, the maximum fluctuation quantity can be obtained:

$$d_1 = (y_B - y_A)/\cos 36.2° = 0.090 \text{ mm},$$

$$d_2 = (y_D - y_C)/\cos 36.2° = 0.058 \text{ mm}.$$

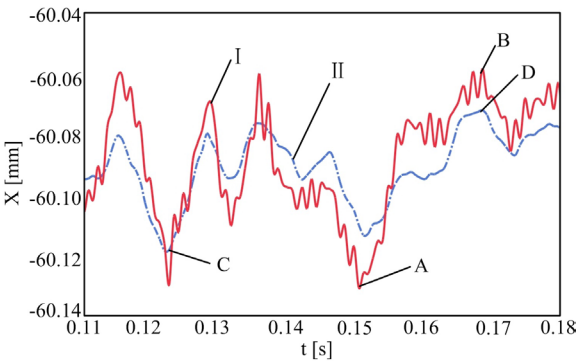

Fig. 12. *Tension sprocket fluctuation along X-axis*

It can be observed that the fluctuation of the dual-phase silent chain system is small. Moreover, the fluctuation of the dual-phase silent chain system is smaller than that of the single-phase silent chain system. Furthermore, it is obvious that the fluctuation of curve I is more drastic than the fluctuation of curve II. So it can be concluded that the transmission of double-side meshing and the dual-phase driving system is steady and credible.

3.2 Link Vibration Analysis

Because of the influence of the chain polygon effect, the impact between the link plates and the sprockets, and the gravity of the chain, transverse vibration, and longitudinal vibration are unavoidable in the process of transmission. In this paper, the link vibration is analysed through researching link trajectory and the rotational speed of a link plate. In Fig. 13, the link trajectory is shown. In Fig. 14, the rotational speed of a link plate is shown, where T_1 and T_2 are two periods of the running.

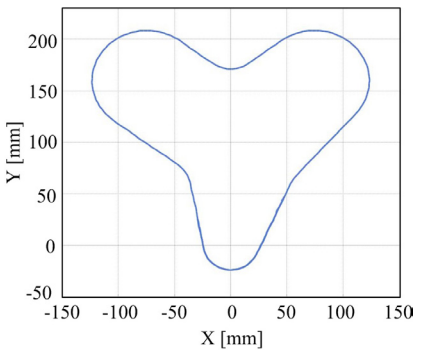

Fig. 13. *The link trajectory*

From Fig. 13, it can be seen that the link trajectory is smooth and steady, and the vibration amplitude is very small. From Fig. 14, it can be seen

that at the beginning of the running, the fluctuation of the rotational speed is bigger and bigger, which is caused by the assembly gap of the system and the effect of the sprocket tension group. During link plate meshing with sprockets, the fluctuation is small, which indicates, according to [16], that the meshing is smooth. In summary, double-side meshing and dual-phase driving timing silent chain system can work smoothly and has little vibration, which can enhance reliability and decrease the noise of the system.

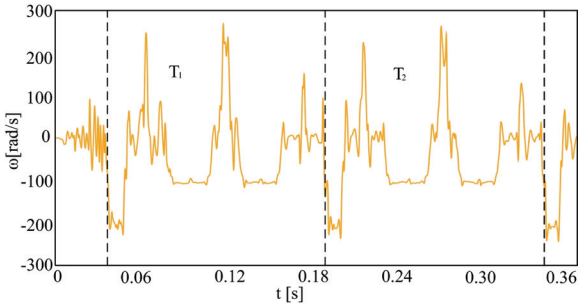

Fig. 14. *The link plate rotational speed*

3.3 Rotational Speed Analysis of Exhaust Camshaft Sprocket

Since the rotational speed of the crankshaft sprocket is constant, the stability of the exhaust camshaft sprocket becomes an important reliability indicator of a silent chain system. The theoretical rotational speed of the exhaust camshaft sprocket is $\omega_2 = \omega_1 / n = 104.72$ rad/s, where ω_1 is the rotational speed of the crankshaft sprocket, and n is the transmission ratio of the exhaust camshaft sprocket and the crankshaft sprocket. As shown in Fig. 15, I is the rotational speed curve of the single-phase silent chain system, and II is the rotational speed curve of a dual-phase silent chain system, and III is the theoretical rotational speed curve.

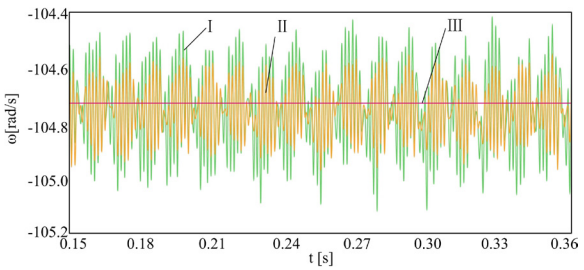

Fig. 15. *The rotational speed of the exhaust camshaft sprocket*

Rotational speed stability index μ is always used to measure the stability of sprocket rotation. Moreover, μ is calculated as:

$$\mu = \Delta\omega / \omega_2, \tag{9}$$

where $\Delta\omega$ is the fluctuation quantity of the rotational speed. From Fig. 15, it can be seen that the tendencies of curve I and II are roughly the same. According to Eq. (9), it can be obtained that the rotational speed stability index of a single-phase silent chain system is 0.66%, the rotational speed stability index of a dual-phase silent chain system is 0.38%, and both of them can meet the design requirements of the system, but the dual-phase silent chain system has better performance than the single-phase silent chain system.

3.4 Transmission Error Analysis

Because of the influence of the chain polygon effect and impact load, the transmission error between exhaust camshaft sprocket and intake camshaft sprocket is unavoidable. As shown in Fig. 16, I stands for the transmission ratio of a single-phase silent chain system, II stands for the transmission ratio of a dual-phase silent chain system, and III stands for the theoretical transmission ratio. Since the intake camshaft sprocket and the exhaust camshaft sprocket have same tooth number, the theoretical transmission ratio is a constant one.

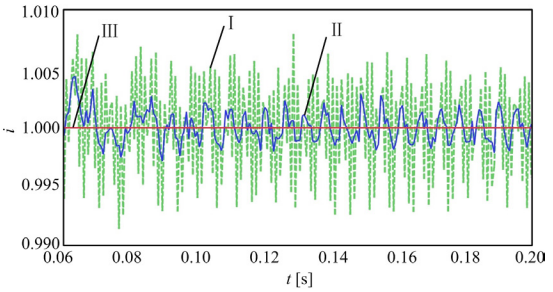

Fig. 16. *The transmission ratio of intake camshaft sprocket and exhaust camshaft sprocket*

From Fig. 16 it can be seen that the tendencies of curve I and curve II fluctuate around straight line III and they are similar. The transmission error of single-phase silent chain system is 0.80%, while the transmission error of the dual-phase silent chain system is 0.43%. It can be concluded that the transmission errors of the two systems are small, and both of them can meet the design requirements of the system. However, the dual-phase silent chain system can work more reliably than the single-phase silent chain system can.

3.5 Contact Force Analysis

The contact force between link plate and other components is shown in Fig. 17. Stage Ⅰ represents the contact force when the link plate contacts the crankshaft sprocket. Stage Ⅱ represents the contact force when the link plate contacts the sprocket tension group. StageⅢ represents the contact force when the link plate contacts the exhaust camshaft sprocket. StageⅣ represents the contact force when the link plate contacts the idle gear group A. Stage Ⅴ represents the contact force when the link plate contacts the intake camshaft sprocket. StageⅥ represents the contact force when the link plate contacts the idle gear group B.

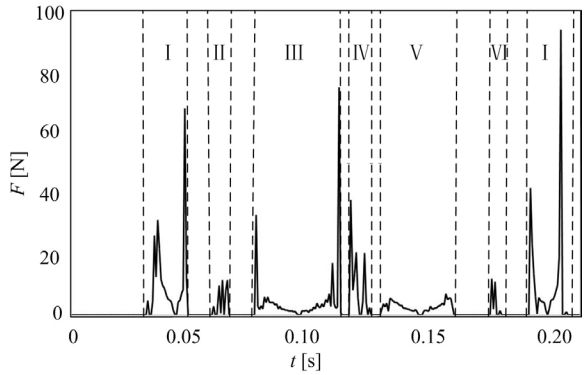

Fig. 17. *The link contact force*

From Fig. 17, it can be seen that the contact force between the link plate and other components is small, which indicates that the double-side meshing and dual-phase driving timing silent chain system can reduce action force and friction between link plates and sprockets and prolong the life of the system. From Stages I, III and V, it can be seen that the contact force is large at the beginning and end of the meshing. This is because that at the beginning of the meshing between the link plate and sprocket, the majority of the load is imposed on the link plate. With the progress of the meshing, the adjacent link plate starts to engage with the sprocket and undertakes an increasing load. Thus, the contact force becomes smaller and smaller. At the end of the meshing, with the former link plate dropping out of the engagement, an increasing load will be imposed on the next link plate.

4 CONCLUSIONS

(1) Based on engine structure, a new type of double-side meshing and dual-phase driving timing silent chain system is designed. Furthermore, a systematic design method of the system is proposed, which lays the theoretical foundation for the design of the engine timing silent chain system.

(2) The fluctuation of the tension sprocket, the vibration of the chain system, the rotation speed stability of the exhaust camshaft sprocket, the transmission error of the intake camshaft sprocket and exhaust camshaft sprocket, and the contact force between link plate and other components are analysed. The analysis results show that the system designed in this paper can meet the performance requirements of the engine timing silent chain system. Furthermore, it verifies the scientific validity and the validity of the design method proposed in this paper.

(3) By comparing the single-phase timing silent chain system, the double-side meshing and dual-phase driving timing silent chain system has less fluctuation of the tension sprocket, and a steadier rotation speed of exhaust camshaft sprocket, and a smaller transmission error of the intake camshaft sprocket and exhaust camshaft sprocket.

5 ACKNOWLEDGEMENTS

The research presented in this paper was supported by Jilin Province Science and Technology Development Plan Item (No. 20150204075GX), and National Natural Science Foundation of China (No. 51305154).

6 REFERENCES

[1] Meng, F., Li, B., Lu, X., Wu, L., Wang, H. (2009). Design method of timing chain system for automotive engine. *Journal of Harbin Institute of Technology*, vol. 41, no. 5, p. 121-124. (in Chinese)

[2] Meng, F., Qu, S., Dong, C. (2012). Multi-variation design method of Hy-Vo silent chain. *Transactions of the Chinese Society of Agricultural Machinery*, vol. 43, no. 2, p. 230-234, **DOI: 10.6041/j.issn.1000-1298.2012.02.044**. (in Chinese)

[3] Meng, F., Feng, Z., Li, C., Yin, D. (2004). Experimental research on the wear mechanisms and temperature and speed characteristics of a new silent chain. *Tribology*, vol. 24, no. 6, p. 560-563. (in Chinese)

[4] Huang, C., Kosasih, L., Huang, C.C. (2005). The tooth contact analysis of round pin jointed silent chains. *ASME International Design Engineering Technical Conferences and Computers and Information in Engineering Conference*, vol. 5, p. 605-613, **DOI:10.1115/DETC2005-84065**.

[5] Xu, L., Yang, Y., Chang, Z., Liu, J. (2010). Dynamic modeling of a roller chain drive system considering the flexibility of input shaft. *Chinese Journal of Mechanical Engineering*, vol. 23, no. 3, p. 367-374, **DOI:10.3901/CJME.2010.03.367**.

[6] Troedsson, I., Vedmar, L. (1999). A dynamic analysis of the oscillations in a chain drive. *Journal of Mechanical Design*, vol. 123, no. 3, p. 395-401, **DOI:10.1115/1.1374196**.

[7] Pereira, C.M., Ambrósio, J.A., Ramalho, A.L. (2010). A methodology for the generation of planar models for multibody chain drives. *Multibody System Dynamics*, vol. 24, no. 3, p. 303-324, **DOI:10.1007/s11044-010-9207-x**.

[8] Wang, Y., Ji, D.S., Zhan, K. (2013). Modified sprocket tooth profile of roller chain drives. *Mechanism and Machine Theory*, vol. 70, p. 380-393, **DOI:10.1016/j.mechmachtheory.2013.08.006**.

[9] Zhang, W. (2005). An analysis on vibration of moving silent chain by multi-body dynamics. *ASME International Design Engineering Technical Conferences and Computers and Information in Engineering Conference*, vol. 6, p. 1707-1712, **DOI:10.1115/DETC2005-85311**.

[10] Xue, Y., Wang, Y., Wang, X. (2006). CAD and machining simulation of involute sprockets. *Journal of Wuhan University of Technology*, vol. 28, no. 5, p. 105-107. (in Chinese)

[11] Xue, Y., Wang, Y., Wang, X. (2007). Engagement theory of silent chain mechanism with involute tooth profile. *Journal of Jiangsu University (Natural Science Edition)*, vol. 28, no. 2, p. 104-107. (in Chinese)

[12] Feng, Z., Meng, F., Li, C. (2005). Meshing mechanism and simulation analysis of a new silent chain. *Journal of Shanghai Jiaotong University*, vol. 39, no. 9, p. 1427-1430. (in Chinese)

[13] Pedersen, S.L., Hansen, J.M., Ambrósio, J.A.C. (2004). A roller chain drive model including contact with guide-bars. Multibody System Dynamics, vol. 12, no. 3, p. 285-301, **DOI:10.1023/B:MUBO.0000049131.77305.d8**.

[14] Pedersen, S.L. (2005). Model of contact between rollers and sprockets in chain-drive systems. *Archive of Applied Mechanics*, vol. 74, no. 7, p. 489-508, **DOI:10.1007/s00419-004-0363-4**.

[15] Cheng, Y., Wang, Y., Li, L., Yin, S., An, L., Wang, X. (2015). Design method of dual phase Hy-Vo silent chain transmission system. *Strojniški vestnik - Journal of Mechanical Engineering*, vol. 61, no. 4, p. 237-244, **DOI:10.5545/sv-jme.2014.2318**.

[16] Calì, M., Sequenzia, G., Oliveri, S.M., Fatuzzo, G. (2015). Meshing angles evaluation of silent chain drive by numerical analysis and experimental test. *Meccanica*, p. 1-15, **DOI:10.1007/s11012-015-0230-0**.